Supplemental Table 1. Necropsy of DN-IkTg mice

A total of 39 organs were examined. Those not mentioned in the table were found to be normal in both the WT and DN-IkTg mice.

Organ	WT	DN-IkTg
Cecum	Normal	Mild, focal GALT hyperplasia
Femur, Marrow	Normal	Minimal, granulocytic hyperplasia
Liver	Minimal, subacute multifocal inflammation	Mild, subacute multifocal inflammation
LN, mandibular	Minimal, bilateral lymphoid hyperplasia	Mild, unilateral histiocytosis Moderate, bilateral lymphoid hyperplasia Mild, bilateral plasmacytosis
LN, mesenteric	Minimal lymphoid hyperplasia	Mild lymphoid hyperplasia Mild Plasmacytosis Mild dendritic cell hyperplasia
Lung	Normal	Minimal, multifocal lymphocytic infiltrate Minimal, focal thrombus
Pancreas	Normal	Minimal, multifocal lymphocytic infiltrate Minimal, focal acinar degeneration
Salivary Gland	Minimal, focal unilateral lymphocytic infiltrate	Mild, multifocal bilateral lymphocytic infiltrate
Spleen	Normal	Mild lymphoid hyperplasia
Thymus	Normal	Focal cysts present Moderate, cortical lymphoid hyperplasia

Supplemental Table 2. Apoptosis pathway PCR gene array

List shows differential gene expression of WT versus DN-IkTg CD4SP cells. Data are representative of three independent experiments.

Gene	Fold Change (over WT)	Gene	Fold Change (over WT)	Gene	Fold Change (over WT)
Bag3	39.0608	Tnfsf12	0.8971	Polb	0.4499
Birc5	3.6666	Trp63	0.8971	Bcl2l1	0.4297
Bid	3.1449	Trp73	0.8971	Dffb	0.4252
Hells	2.5608	Xiap	0.8732	Cflar	0.4103
Casp3	2.0605	Bok	0.8452	Bnip3	0.3841
Naip2	1.8295	Sphk2	0.8324	Birc2	0.3527
Apaf1	1.6906	Bnip2	0.8169	Casp6	0.3296
Cd40	1.6772	Tnfrsf10b	0.7886	Casp7	0.3207
Atf5	1.6441	Trp53	0.7818	Cradd	0.3144
Nol3	1.5649	Zc3hc1	0.7727	Mcl1	0.3108
Tnfsf10	1.4166	Casp4	0.7664	Casp9	0.309
Prdx2	1.3715	Tsc22d3	0.7639	Bnip3l	0.2736
Bad	1.1356	Rnf7	0.7544	Bcl10	0.2324
Bax	1.0949	Api5	0.7487	Pycard	0.2246
Hprt1	1.0409	Bak1	0.7418	Tnf	0.2046
Traf2	1.0266	Akt1	0.722	Traf3	0.2025
Bcl2l2	0.9757	Dad1	0.7173	Tnfrsf1a	0.2008
Bcl2l10	0.8971	Gusb	0.7056	Fasl	0.1893
Card10	0.8971	Cd70	0.6982	Nfkb1	0.1787
Casp1	0.8971	Trp53bp2	0.6862	Casp8	0.1437
Casp12	0.8971	Bag1	0.6665	Cd40lg	0.1312
Casp14	0.8971	Fadd	0.6126	Pim2	0.1214
Cidea	0.8971	Cideb	0.5391	Dapk1	0.1196
Il10	0.8971	Trp53inp1	0.5389	Birc3	0.1123
Lhx4	0.8971	Casp2	0.5326	Card6	0.0727
Naip1	0.8971	Ltbr	0.5274	Traf1	0.071
Nme5	0.8971	Dffa	0.5043	Bcl2	0.0682
Pak7	0.8971	Ripk1	0.4876	Fas	0.0388
Tnfrsf11b	0.8971	Nod1	0.4729		

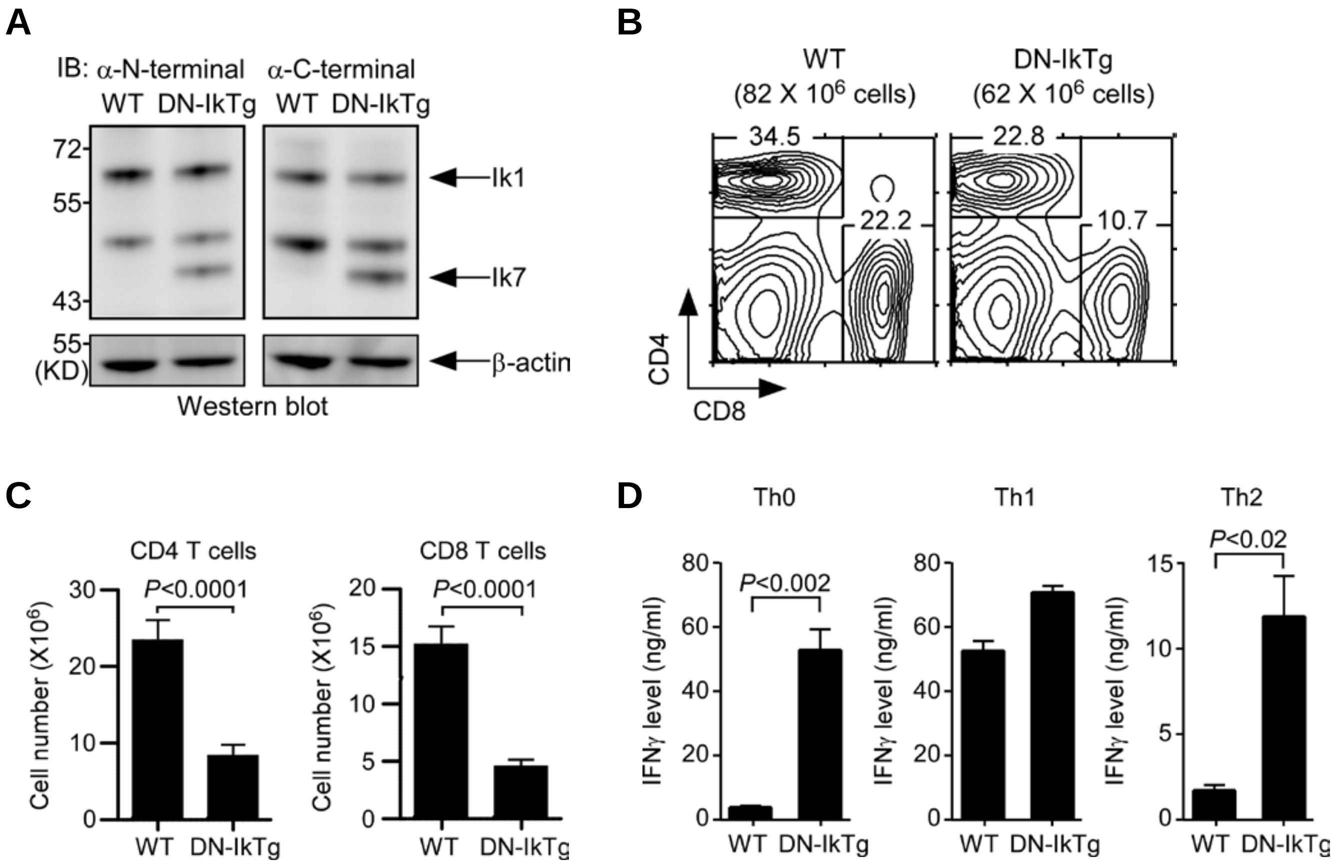

Supplemental Figure 1. Transgenic DN-Ikaros expression in peripheral T cells.

(A) Immunoblot analysis of WT and DN-IkTg LN T cells. Whole T cell lysates were probed with Ikaros N-terminal (left) or C-terminal (right) specific antibodies. The same blot was reprobed with anti-β-actin antibodies as loading control. Blots are representative of 3 independent experiments with 3 WT and 3 DN-IkTg mice.

(B) LN cell profiles of WT and DN-IkTg mice. CD4, CD8 profiles and total cell numbers were determined in single cell suspensions of WT and DN-IkTg LN cells. Data are representative of 8 independent experiments with each one WT and one DN-IkTg mouse.

(C) Peripheral LN T cell numbers of WT and DN-IkTg mice. Data are the summary of 8 independent experiments with each one WT and one DN-IkTg mouse. Bar graphs show mean number ± SEM.

(D) *In vitro* T helper cell differentiation of WT and DN-IkTg $CD4^+$ T cells. Purified $CD4^+$ LNT cells were stimulated under Th0, Th1, or Th2 conditions for 5 days. IFNγ levels in culture supernatants were measured by ELISA. Bar graphs show mean ± SEM from three independent experiments.

Suppl. Figure 2

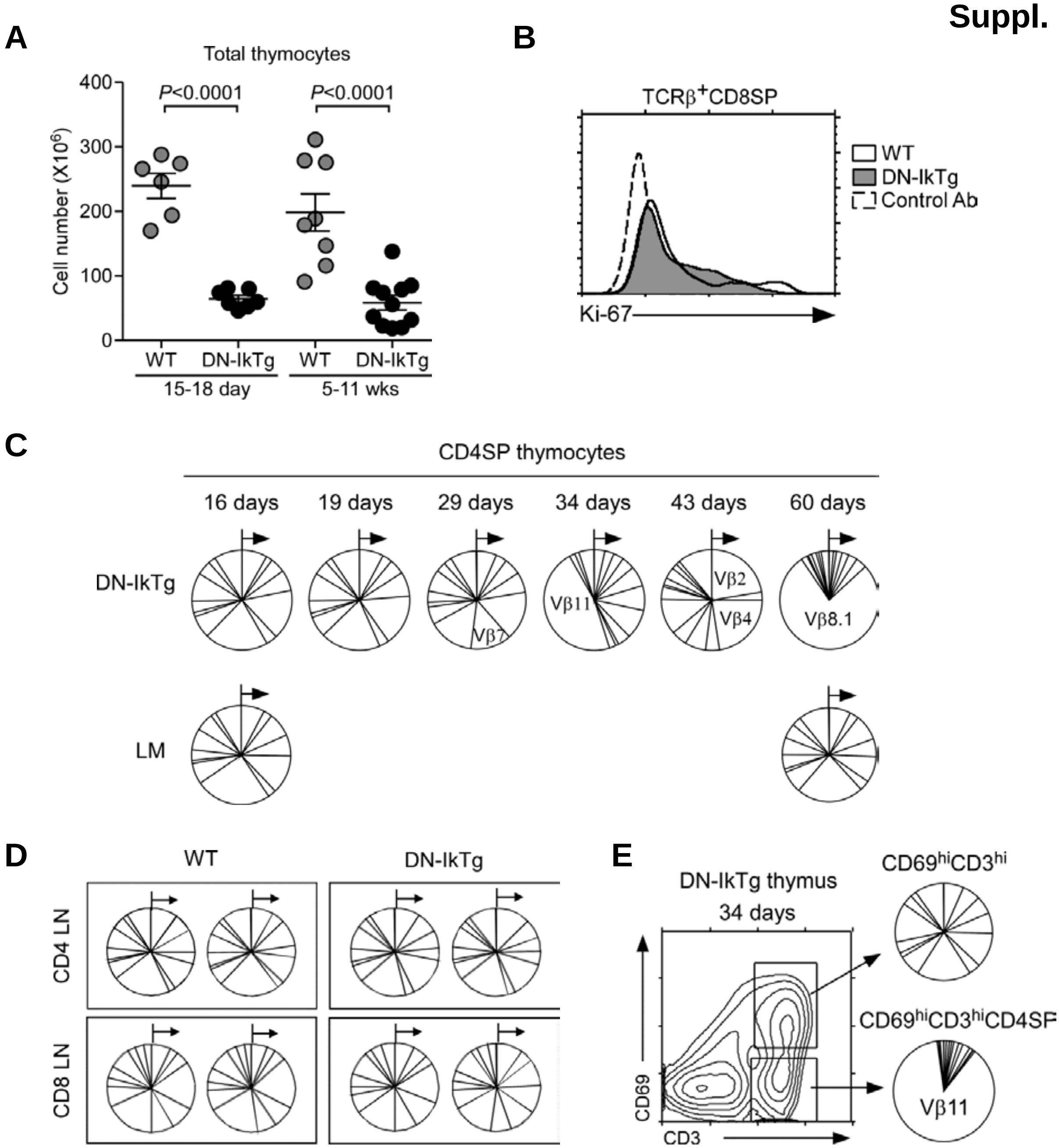

Supplemental Figure 2. TCR Vβ distribution in $CD4^+$ and $CD8^+$ LNT cells.

(A) Thymocyte numbers in neonate and adult DN-IkTg mice. Total thymocyte numbers were determined at indicated age. Each circle corresponds to an individual mouse.

(B) Intracellular Ki-67 staining of WT and DN-IkTg $TCR\beta^+$ CD8SP thymocytes. Histogram is representative of three independent experiments with 4 WT and 6 DN-IkTg mice.

(C) TCR Vβ analysis of littermate (LM) and DN-IkTg CD4SP thymocytes with progressing age. CD4SP cells from indicated mice were stained for a panel of 15 different TCR Vβ, starting from Vβ2 through $V\beta17^a$ in clockwise direction (Materials and Methods). Relative expression of individual TCR Vβ chains are shown in pie charts for each individual mouse. Each chart represents an independent experiment.

(D) TCR Vβ analysis of WT and DN-IkTg LNT cells. TCR Vβ analysis with $CD4^+$ and $CD8^+$ LNT cells are shown in pie charts.

(E) TCR Vβ analysis of the indicated thymocyte subpopulations in DN-IkTg mice. Total thymocytes were stained for CD69 and CD3, followed by CD4/CD8 analysis to assess TCR Vβ distribution

Suppl. Figure 3

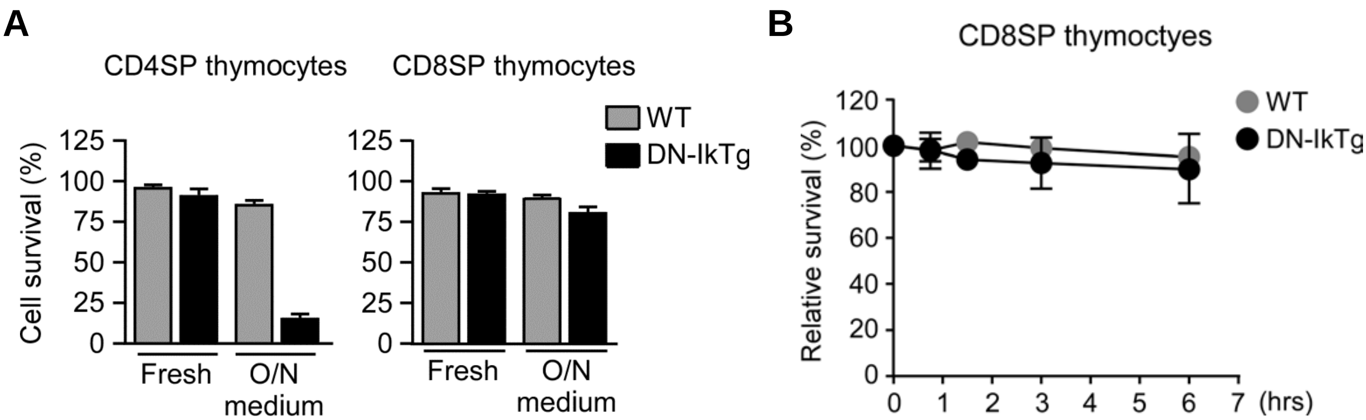

Supplemental Figure 3. DN-IkTg induces apoptosis in CD4SP thymocytes.
(A) Cell viability of freshly isolated versus overnight medium incubated DN-IkTg SP thymocytes. WT and DN-IkTg CD4SP and CD8SP thymocytes were assessed for cell survival by propidium iodide exclusion at indicated time points. Graph shows mean ± SEM from three independent experiments with 3 WT and 6 DN-IkTg mice.
(B) Survival kinetics of WT and DN-IkTg CD8SP thymocytes *in vitro*. Data show the summary of three independent experiments with 3 WT and 6 DN-IkTg mice.

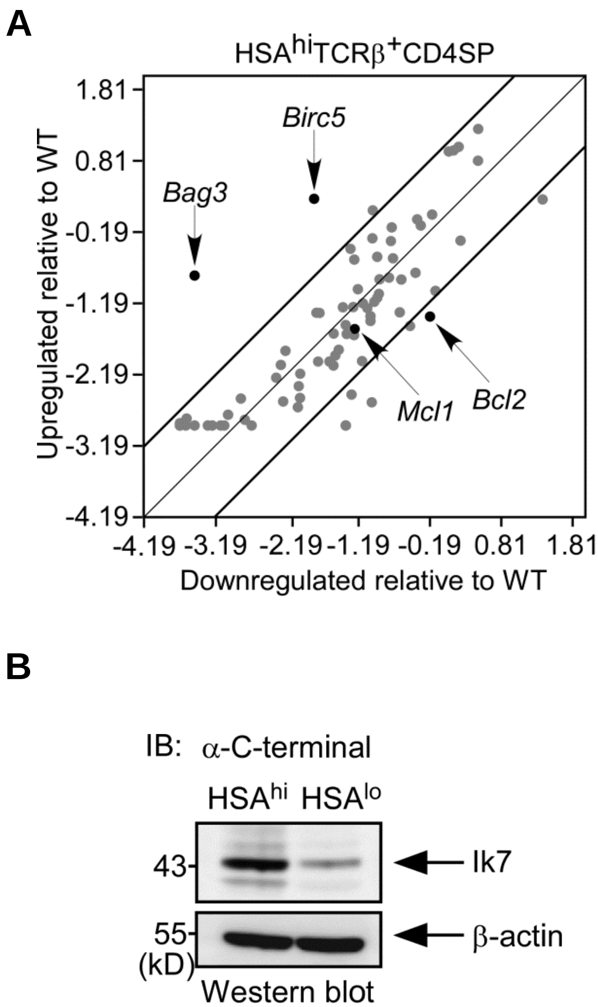

Supplemental Figure 4. Developmentally distinct expression of pro-survival molecules in DN-IkTg thymocytes

(A) Apoptosis pathway gene array analysis of sorted thymocyte subpopulations from WT and DN-IkTg mice. Total RNA from sorted WT or DN-IkTg cells were used to probe PCR arrays for expression of pro- and anti-apoptotic genes. Data are representative of two independent experiments using sorted CD4SP thymocytes from each 3 WT and 3 DN-IkTg mice.

(B) Immunoblot analysis of DN-IkTg expression. Whole cell lysates from sorted HSA^{hi} and HSA^{lo} TCRβ^{+} DN-IkTg thymocytes were assessed for transgenic DN-IkTg expression. The same blot was reprobed with anti-β-actin antibodies for loading control. Blot is representative of three independent experiments.

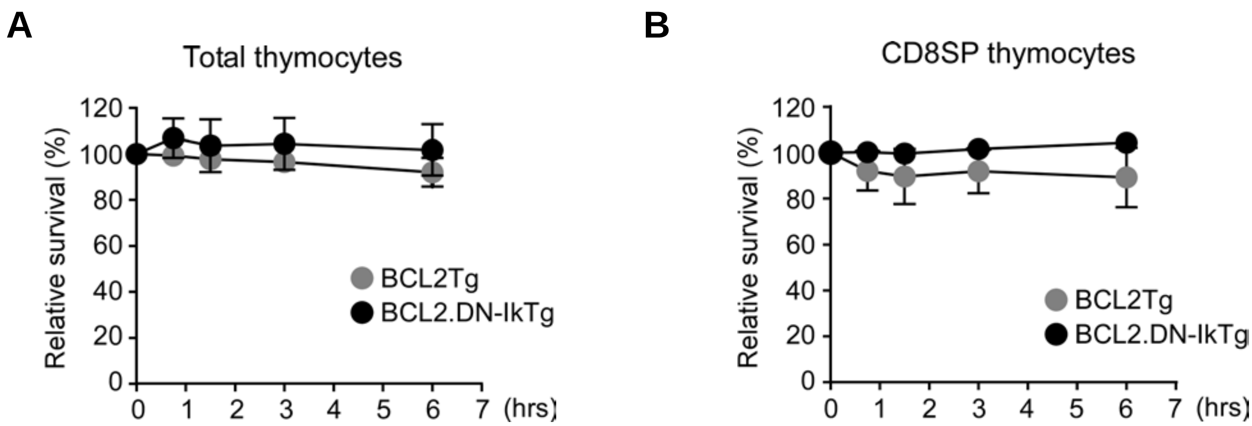

Supplemental Figure 5. Transgenic Bcl-2 rescues programmed cell death in DN-IkTg thymocytes.
(A) Survival kinetics of BCL2Tg and BCL2.DN-IkTg total thymocytes *in vitro*. Data show the summary of three independent experiments
(B) Survival kinetics of BCL2Tg and BCL2.DN-IkTg CD8SP thymocytes *in vitro*. Data show the summary of three independent experiments.

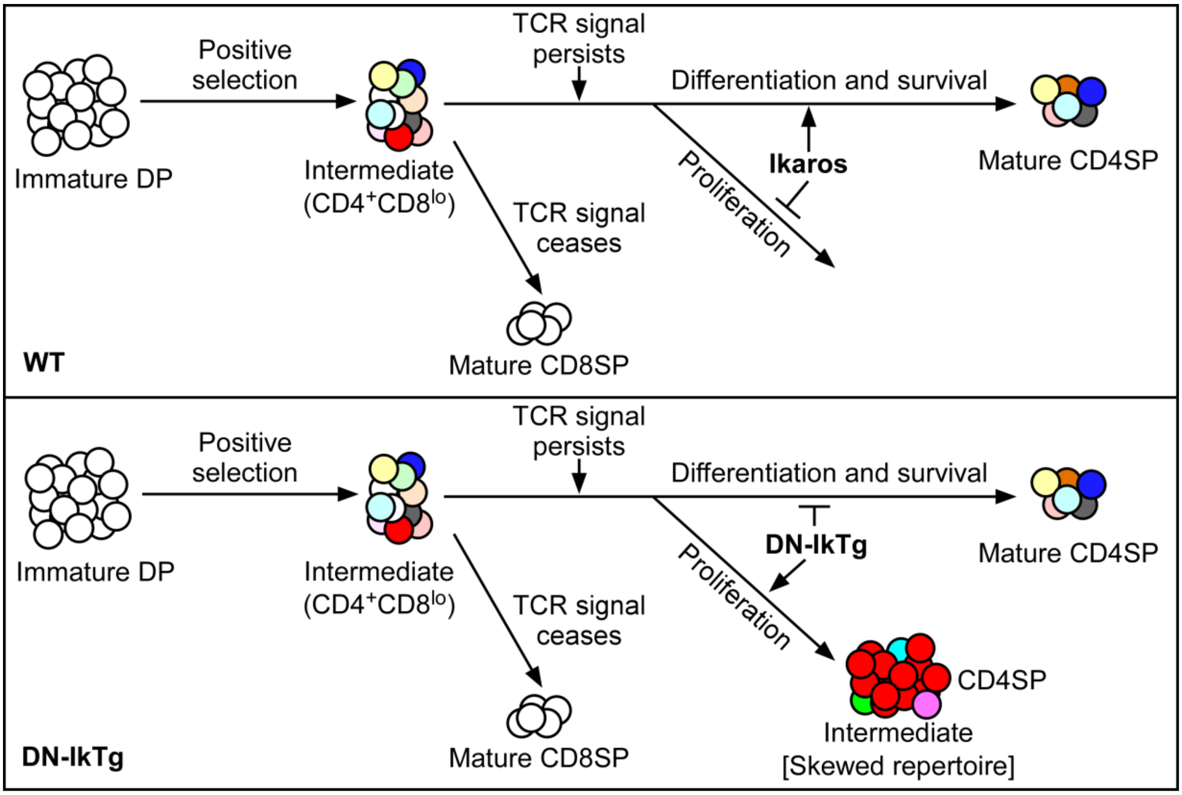

Supplemental Figure 6. Ikaros controls the outcome of selecting TCR signals during thymocyte development

$CD4^+CD8^{lo}$ intermediate cells can be generated by either MHCI or MHCII engagement of the TCR. However, the conspicuous absence of CD4SP cells in MHCIIKO.DN-IkTg mice revealed that DN-IkTg CD4SP cells were mostly dependent on MHCII. This raises the question why MHCI-specific TCR signals fail to induce accumulation of intermediate cells in DN-IkTg mice. According to the kinetic signaling model, persistent TCR signals such as in TCR/MHCII engagements will impose CD4 lineage choice while cessation of positive selecting TCR signals such as in TCR/MHCI engagements will drive CD8 lineage differentiation . Thus, TCR signaling in MHCI-specific $CD4^+CD8^{lo}$ intermediate cells will be terminated upon positive selection and Ikaros function is not further required to control downstream effects of TCR signals (**top**). On the other hand, TCR signaling in MHCII-specific $CD4^+CD8^{lo}$ intermediate cells will persist, and according to our results, it is the persistent TCR signaling that drives the clonal expansion and accumulation of intermediate cells in DN-IkTg thymocytes. Therefore, Ikaros function is required to constrain persistent TCR signals from inducing proliferation and apoptosis of MHCII-signaled $CD4^+CD8^{lo}$ intermediate cells (**bottom**).